

Article

## Carbon Materials from Lignin and Sodium Lignosulfonate via Diisocyanate Cross-Linking and Subsequent Carbonization

Sebastian P. Leitner <sup>1,\*†</sup>, Günther Gratzl <sup>1,†</sup>, Christian Paulik <sup>2</sup> and Hedda K. Weber <sup>1</sup>

<sup>1</sup> Kompetenzzentrum Holz GmbH, Altenberger Str. 69, 4040 Linz, Austria;

E-Mails: g.gratzl@kplus-wood.at (G.G.); h.weber@kplus-wood.at (H.K.W.)

<sup>2</sup> Johannes Kepler University Linz, Institute for Chemical Technology of Organic Materials, Altenberger Str. 69, 4040 Linz, Austria; E-Mail: christian.paulik@jku.at

† These authors contributed equally to this work.

\* Author to whom correspondence should be addressed; E-Mail: s.leitner@kplus-wood.at; Tel.: +43-732-2468-6778; Fax: +43-732-2468-6755.

Academic Editor: Craig E. Banks

Received: 3 August 2015 / Accepted: 16 October 2015 / Published: 23 October 2015

---

**Abstract:** Applications for lignin and lignosulfonates are limited today due to the undefined structure and varying properties of the substance. However, lignin, as the second most abundant bio-resource besides cellulose and the bio-resource with one of the highest natural carbon contents, has the potential to act as a precursor for carbon materials. In this study we have applied a Kraft lignin and a sodium lignosulfonate with the cross-linker toluene-2,4-diisocyanate. The reaction mixture was molded to form small cylindrical shaped paddings. Cross-linked lignin-polyurethane and lignosulfonate-polyurethane networks were analyzed via elemental analysis and thermogravimetric analysis and finally carbonized. The carbon material was analyzed for its BET surface area and its surface structure via scanning electron microscopy. Surface areas between 70 and 80 m<sup>2</sup>·g<sup>-1</sup> could be reached. Moreover, the material was tested for its adsorption potential of crude oil from water and could take up to twice its own weight. For better understanding of the core chemistry of the cross-linking reaction, we have studied the reaction with model substances to define the reactive groups and the influence of sulfonate groups in the cross-linking reaction of lignin and lignosulfonates with toluene-2,4-diisocyanate.

**Keywords:** lignin; lignosulfonate; isocyanate; polyurethane; carbon material; oil adsorption

---

## 1. Introduction

Lignin is one of the main components of wood and a side product of the pulp industry, with a production volume of about 70 million metric tons per year [1]. Today, lignin has only a few low-value applications and it is burned to 95% for energy production [1]. However, lignin is the only natural product with aromatic functionalities which is available in huge quantities [2]. In addition to its aromatic nature, lignin contains different functional groups such as hydroxyl groups (phenolic and aliphatic), ether-bridges and methoxyl groups [1]. In the case of sulfite pulping, lignin is sulfonated during the process and therefore contains sulfonate groups as well. Depending on the origin, lignin differs in its functional group composition and molecular size. Therefore, it can be said that lignin has a hardly definable molecular structure, which complicates its applicability. Nonetheless, the aromatic-nature of lignin makes it the renewable resource with the highest natural carbon content [2], which qualifies it as a promising candidate for carbon materials from a renewable resource.

Carbon materials are frequently discussed in the context of composite materials for polymers [3–5], super capacitors [6,7], electrode materials [8–10] and adsorbing materials [11–13]. In all of these cases, one critical point is the formation of a 3D structure of lignin to introduce orientated structures or pores into the material [8,14,15]. This cross-linking reaction is often performed by introducing radical oxygen species via oxidative thermostabilization. These have unpredictable cross-linking behavior and influence the final quality of the carbonized material [3]. In addition, lignin, as a natural substance, appears in various forms, which have an impact on the final quality of a carbonized material [3]. Therefore, a controllable cross-linking-reaction with defined functional groups of lignin would have advantages in terms of quality in a production process of carbon materials with lignin as a natural precursor. Some authors have reported lignin cross-linking with formaldehyde [16–19], diisocyanates [20–23] and ester-type cross-linked epoxy resins [24] focusing on different material properties, while the resulting carbon material of cross-linked lignin and lignosulfonates, especially with diisocyanates, is poorly studied in literature to date [25].

In this study, we present the formation of 3D cross-linked structures from a lignin and a lignosulfonate with toluene-2,4-diisocyanate (TDI) and a subsequent carbonization reaction, which result in form-stable carbon materials. The cross-linking reaction of the material was studied with NMR spectroscopy and model substances to describe the reactivity of the functional groups of the lignin and the influence of the sulfonate group in the cross-linking reaction, which, to our knowledge, is not described in the literature so far. The advantage of the present method is the solvent-free reaction of solid lignin with a liquid cross-linker. Finally the carbon material was investigated for its surface area and its applicability as an adsorbing agent for crude oil.

## 2. Results and Discussion

### 2.1. Cross-Linking Reaction Study with Model Substances

The cross-linking reaction in this study was performed with TDI and Kraft lignin or lignosulfonate and can be described through the use of model substances. The model substances used are phenol, anisole, benzylalcohol, 4-hydroxybenzylalcohol (HBA), vanillyl alcohol (VA), syringyl alcohol (SA), sodium methanesulfonate (SMSA) and the cross-linker (TDI). These are presented in Figure 1 and <sup>1</sup>H NMR

spectra of the substances can be found in the supplemental information. The model substances were chosen to describe possible reactions of TDI with all available functional groups of lignin, which are aliphatic OH groups, phenolic OH groups, methoxyl groups, and, in the case of lignosulfonates, sulfonate groups. HBA, VA and SA should represent the H- (hydroxyphenyl), G- (guaiacyl) and S- (syringyl) building block units of lignin. All model reactions were performed in solution with a deuterated solvent heated to 60 °C for 24 h. The reaction solutions were then analyzed by  $^1\text{H}$  NMR spectroscopy.

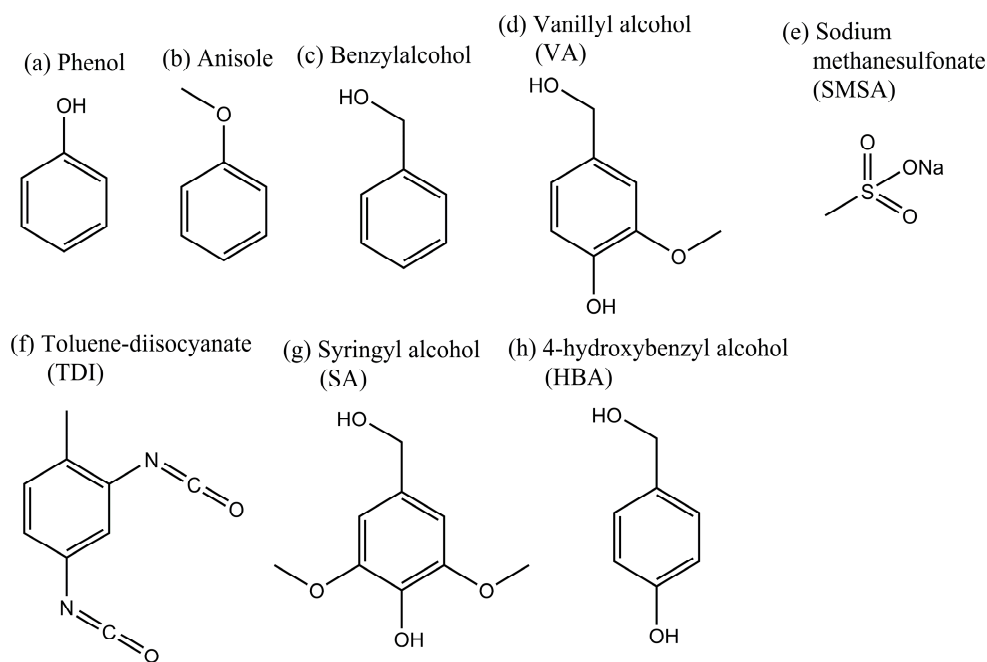
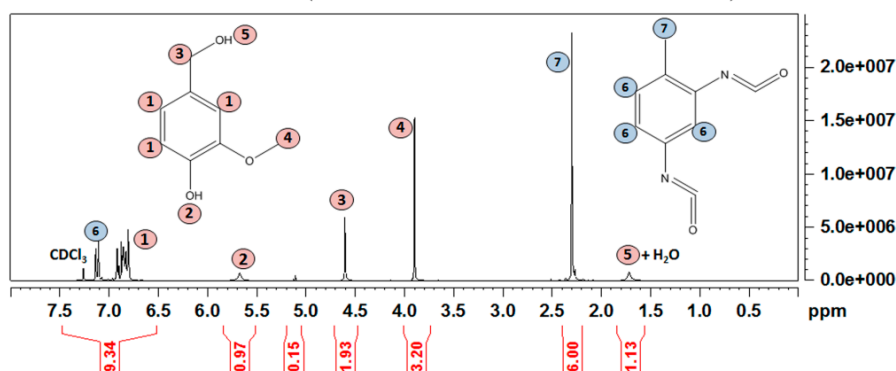


**Figure 1.** Model substances used for describing the influence and the reactivity of functional groups in lignin and lignosulfonates.

Figure 2 shows the  $^1\text{H}$  NMR spectra of the model substance VA, which contains all the important functional groups of lignin, together with TDI (all other reaction processes with model substances can be found in the supplemental information). VA represents the most common lignin building block present in softwood lignins. The reaction of VA with TDI was performed with a double molar amount of TDI to ensure an excess of TDI compared to the functional groups of VA. The observable signals in the  $^1\text{H}$  NMR spectra were assigned by the monomer spectra and after comparisons to a spectra database [26]. After 10 min reaction time at 60 °C (Figure 2a), the spectrum can hardly be differentiated from an overlay of the monomer spectra, except a small, single signal which appears at 5.13 ppm. This signal grows considerably after 24 h reaction time at 60 °C (Figure 2b), while the signal of the CH<sub>2</sub> group of VA at 4.60 ppm drastically decreases. The reaction is also indicated by a decreasing signal of the aliphatic OH group of VA at 1.73 ppm in Figure 2b compared to Figure 2a. As a consequence of the reaction, an NH signal appears, which can be found in the region between 6.50 ppm and 7.50 ppm. In addition, the observed peak shifts of Figure 2 are also in good accordance with the peak shifts of the model substance benzyl alcohol with TDI (supplemental information), which indicates the activity of aliphatic OH groups. The other two functional groups of VA (phenolic OH and the methoxy group) hardly show any reactivity. In case of the methoxy group a reaction was highly unexpected and also not observable, while the signal of the phenolic OH group at 5.70 ppm had a slight decrease in the integral

from Figure 2a to Figure 2b, which can be interpreted as a minor reactivity of the functional group. Nevertheless, the low reactivity of the phenolic OH group was surprising since phenolic OH groups are often used for technical PUs. The difference in this case could be the absence of a catalyst, which is frequently used in PU productions. From these results it can be concluded that lignin cross-links with TDI mostly via its aliphatic OH groups in the absence of a catalyst.

(a)  $^1\text{H}$  NMR spectrum of vanillyl alcohol with TDI after 10 min at  $60^\circ\text{C}$  (double molar amount of TDI)



(b)  $^1\text{H}$  NMR spectrum after 24 h at  $60^\circ\text{C}$  (double molar amount of TDI)

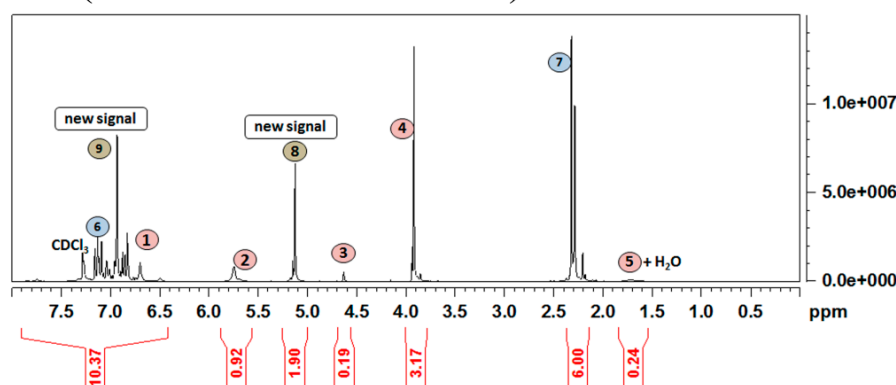


**Figure 2.** Reaction sequence of TDI with VA after (a) 10 min at  $60^\circ\text{C}$  and (b) 24 h at  $60^\circ\text{C}$ . In (c) the greatest possible reaction of TDI with the aliphatic OH group in the absence of a catalyst is shown. (300 MHz, in  $\text{CDCl}_3$ ).

To test the reactions also from other lignin sources, further building blocks were tested in terms of their reactivity with TDI. HBA was used as a model compound for the H-lignin and SA for the S-lignin. Similar to the investigations of VA, the compounds were studied by NMR measurements in  $\text{DMSO-d}_6$  as solvent.

HBA showed such a high reactivity that after ten minutes of reaction time at  $60^\circ\text{C}$ , only a gel was present, which made a liquid  $^1\text{H}$  NMR measurement impossible. IR spectroscopy of the formed gel showed that significant urethane absorption bands showed up at  $3304.82\text{ cm}^{-1}$  from the N-H stretching, and also at  $1712.61\text{ cm}^{-1}$  from the carbonyl group. Nevertheless, combined with the reactivity measurements (supplemental information) of phenol, which showed no reaction without catalyst, and the reactivity of benzylalcohol, it can be assumed that the aliphatic hydroxyl group is the most reactive group and the aromatic hydroxyl group is a possible attacking site for a fast crosslinkage.

Syringyl alcohol should be a model compound for the S-lignin building block. The relevant NMR spectra are added in the supplemental information. Similar to the results from the VA reaction, both OH groups and the CH<sub>2</sub> group are most relevant for the reaction observation. In DMSO-d<sub>6</sub> as solvent, the CH<sub>2</sub> group can be found at 4.39 ppm, the aliphatic OH group at a very broad and not very intensive peak at 5.03 ppm and the phenolic OH at 8.15 ppm. After 24 h at 60 °C reaction temperature, similar to the experiment with VA, two new signals are formed while the signals from the aliphatic chain almost completely disappear. The first new signal can be attributed to the new CH<sub>2</sub> signal directly next to the newly formed urethane group, which is shifted to 5.11 ppm. The original methylene signal disappeared. A second new peak appears at 6.80 ppm, which should be an indicator for a new NH group, formed in the urethane network. The reaction of the vanillyl alcohol with TDI proceeds faster than the respective reaction of syringyl alcohol. Previous work on this topic by Zhunag *et al.* also shows that the aliphatic OH group is more reactive to isocyanates than the phenolic OH group [27].

Testing of the sulfonate groups was more intricate, since the solubility was lower. Due to the pulping process, sulfonation of lignin exclusively provides sulfonate groups attached to aliphatic chains and not to aromatic carbons [28]. We found that the sodium salt of methanesulfonic acid does not react with TDI due to the absence of an acidic OH-group. During the tests, the water content turned out to be of main importance, as it is shown with the model substance SMSA. It is observable that the sulfonate group of SMSA does not react with the isocyanate group of TDI. However, the water signal (3.38 ppm) in the reaction solution completely disappears due to the reaction of water with TDI. From these observations it can finally be concluded that lignosulfonates are cross-linked via a catalyzed reaction of their OH groups and TDI, with sulfonate groups as a catalyst.

## 2.2. Carbonization of Cross-Linked Kraft Lignin or Lignosulfonates

LPUs (Lignin polyurethane; Kraft lignin plus TDI) and LSPUs (Lignosulfonate polyurethane; lignosulfonate plus TDI) were derived from a solvent-free synthesis (60 °C, 24 h). After 24 h reaction time, the materials were transferred to ceramic containers for subsequent pyrolysis.

The carbonization reaction was performed at a maximum temperature of 900 °C. For this temperature it is reported that the physical structure of the material hardly changes, while the pyrolysis reactions causes carbonization of the material [29,30]. For the carbonization reaction the weight loss was determined thermogravimetrically, which is shown in Figure 3.

It can be seen that pyrolysis of LPUs and LSPUs is a multistep reaction, described in detail in the literature [31–35]. The measured terminal residue weight of different LSPU samples varies between 34.3% (LSPU 1), 30.5% (LSPU 2) and 28.7% (LSPU 3). Similar to that the LPU samples show a range of residue weight from 31.5% (LPU 1) to 28.1% (LPU 2) and 28.6% (LPU 3). Thermograms of the initial material lignin and lignosulfonate look very similar to the produced polyurethanes, although the starting temperature of the main decomposition is shifted to slightly lower temperatures in the products. Also, the residual carbon weight of the resource materials is with 40% to 42% slightly higher.

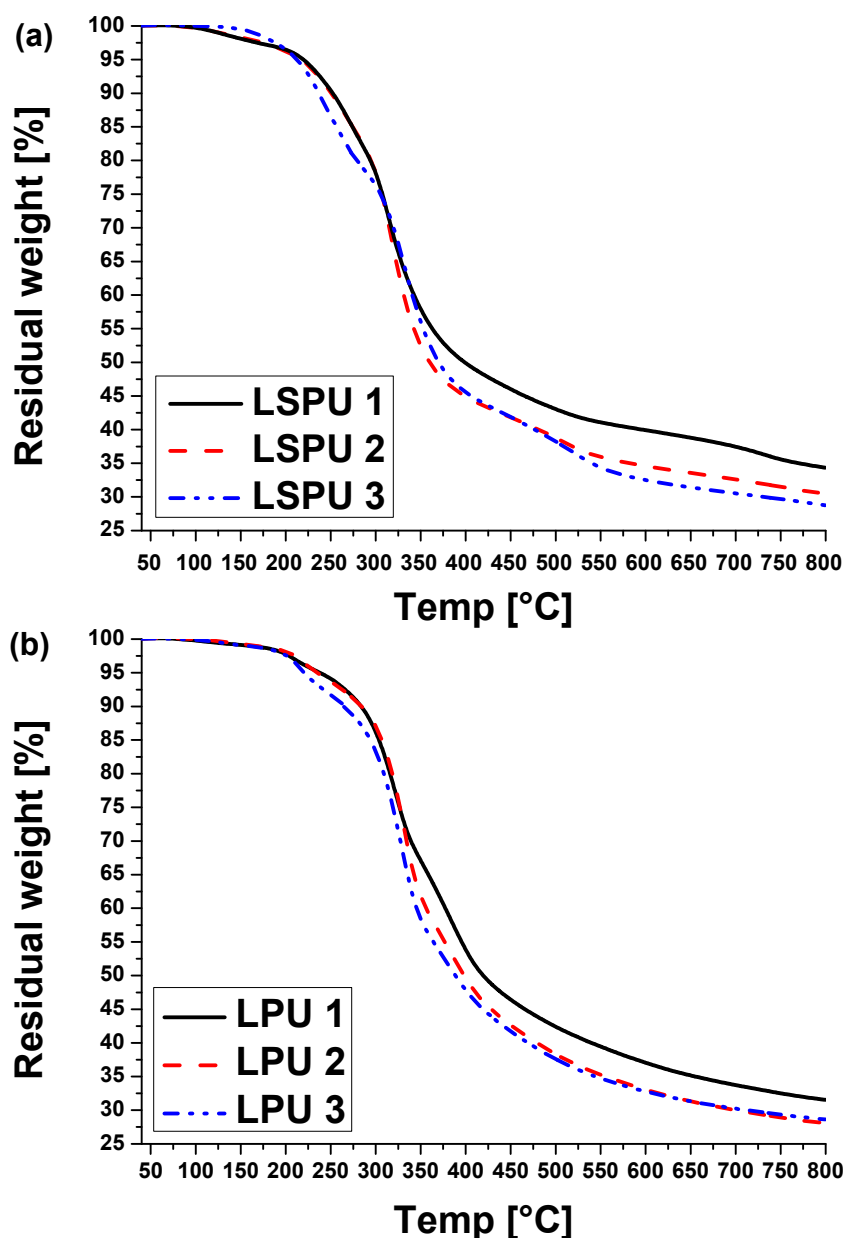


**Figure 3.** TGA curves of (a) LSPU samples and (b) LPU samples. ( $10\text{ }^{\circ}\text{C}\cdot\text{min}^{-1}$ ,  $\text{N}_2\text{ }20\text{ mL}\cdot\text{min}^{-1}$ ).

The calculated initial carbon contents of the LPU and the LSPU (calculation based on the composition determined by elemental analysis in Table 3 and TDI) as well as the analytically determined carbon contents are summarized in Table 1. It can be seen that the final weights of carbonized LPUs as well as carbonized LSPUs (Table 1) do not reach the theoretical value due to volatile carbon-containing fractions [34].

To improve the formation of carbon and reduce the production of volatile hydrocarbons, the thermal carbonization reaction was performed with only a slow increase in temperature [1]. From the results of elemental analysis it seems that LSPU residues have a lower carbon loss compared to the LPU samples, since they have a comparable residue but a lower initial carbon content. Lignosulfonate materials show higher ash content than the Kraft lignin, which could be a reason for that. The inorganics residue (ash) in the carbon material seems to increase the carbon content because it does not decompose during the pyrolysis process under inert gas atmosphere [28].

The ash can be observed in the form of nano-sized-needles on the surface of the lignosulfonate-based carbon material and is presented in Figure 4a,b. In case of lignin-based carbon materials, salt-crystals cannot be found (Figure 4c,d). As a consequence of the salt appearance in the carbon material, a difference in the behavior in water can be found. While LPUs are floating, LSPUs are sinking in water. This behavior of the material can be correlated with the properties of the salt crystals, which are highly dense and distribute water throughout the material due to their hydrophilic character.

**Table 1.** LPU and LSPU compositions according to the results from elemental analysis.

Name	Initial Composition TDI:Lignin or TDI:Lignosulfonate (g:g)	Elemental Analysis				Residue after TGA-Carbonization (wt%)
		C ( $C_{calc}$ ) * (wt%)	H ( $H_{calc}$ ) * (wt%)	N ( $N_{calc}$ ) * (wt%)	S ( $S_{calc}$ ) * (wt%)	
LPU 1	0.5	62 (61)	4.9 (4.7)	6.8 (5.4)	-	32
LPU 2	1.0	62 (62)	4.8 (4.4)	9.2 (8.0)	-	28
LPU 3	1.5	62 (62)	4.7 (4.2)	10 (9.7)	-	28
LSPU 1	0.5	48 (48)	4.3 (4.1)	5.5 (5.4)	2.9 (2.6)	34
LSPU 2	1.0	53 (51)	4.5 (3.9)	9.1 (8.0)	2.6 (1.9)	30
LSPU 3	1.5	56 (53)	4.2 (3.8)	11 (9.7)	2.2 (1.5)	29

\*  $C_{calc}$ ,  $H_{calc}$ ,  $N_{calc}$  and  $S_{calc}$  are calculated contents from the TDI:LPU and TDI:LSPU compositions based on the elemental analysis results from lignin and the lignosulfonate results of Table 3 and the composition of TDI.

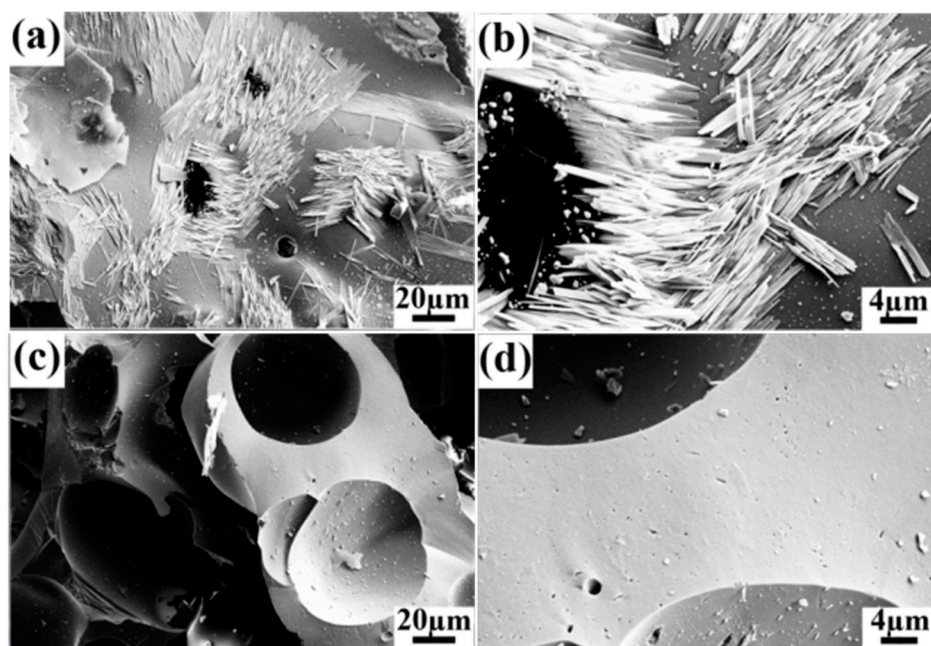


**Figure 4.** Comparison of different product materials. (a) and (b) SEM images of LSPU 3 showing nano-salt-crystals; (c) and (d) SEM images of LPU 3 showing a smooth surface without crystals.

### 2.3. Carbon Material

The carbon material was investigated in terms of its BET surface area and its applicability for its use as adsorbent. The BET surface area of the carbon materials is presented in Table 2. We observed that

the largest surface area can be found within the samples LPU 2 and LSPU 2, which initially had the same composition of lignin or lignosulfonate and TDI.

**Table 2.** BET surface areas, elemental analysis and densities of carbonized LPUs and LSPUs.

Carbonized Material	Elemental Analysis			Bulk Density ( $\text{g}\cdot\text{cm}^{-3}$ )	BET Surface Areas ( $\text{m}^2\cdot\text{g}^{-1}$ )
	C (wt%)	H (wt%)	N (wt%)		
LPU 1	85	0.8	2.9	0.145	9.64
LPU 2	87	0.9	3.1	0.153	80.3
LPU 3	85	0.8	3.3	0.132	0.86
LSPU 1	68	0.8	1.1	0.520	42.8
LSPU 2	65	0.8	0.9	0.492	70.8
LSPU 3	67	0.9	1.1	0.501	1.51

**Table 3.** Lignin and lignosulfonate compositions according to the results from elemental analysis (based on dry matter).

Name	Elemental Analysis		
	C (wt%)	H (wt%)	S (wt%)
Lignin	61	5.3	-
Lignosulfonate	40	4.4	3.8

Hence, the differences in the surface area can also be found in the surface structure. In Figure 4a–d the smooth surfaces of LSPU 3 (Figure 4a,b) and LPU 3 (Figure 4c,d) are shown. In contrast, the rougher surfaces of Figure 5, showing the surface structures of LSPU 2 (Figure 5a) and of LPU 2 (Figure 5b), indicate larger surface areas. As it can be observed from Figure 5, beside rougher surface structures, quite smooth areas are also present, which finally result in a limitation in the surface area size. It seems that areas with higher and lower cross-linking degrees are present throughout the surface, which produces rougher and smoother structures.

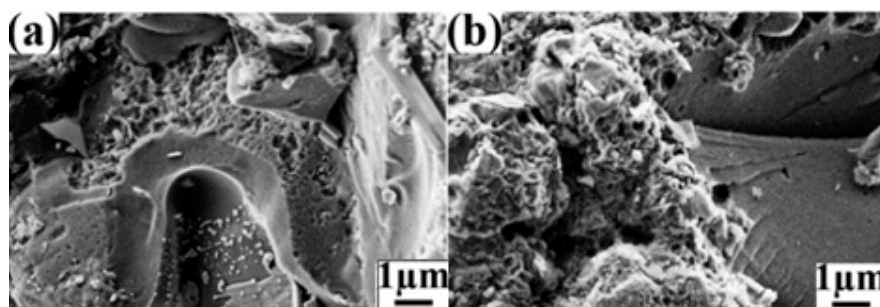


**Figure 5.** SEM images indicating the surface structures of carbonized (a) LSPU 2 and (b) LPU 2.

Finally, the carbon materials were investigated for their ability to adsorb crude oil. Therefore, we mixed water with crude oil and added a certain amount of the carbonized material. After shaking for some time, the amount of crude oil decreased and was adsorbed by the carbon material as shown in Figure 6. In Figure 7 the relative mass increase of different samples of the produced polyurethane material is

plotted against the time. As can be seen, this increase is significantly higher compared to the sample in pure water. A maximum crude oil uptake could be estimated at about 20 to 30 min. The material is able to increase its own weight by 200% while there was almost no visible change in dimensions. We therefore suggest the carbon materials as a possible adsorbent for crude oil in water. The suitability is comparable to other materials used in oil adsorption [36]. A potential way to recycle the carbon material again is simple burning of the crude oil and reuse of the materials or vacuum filtration.

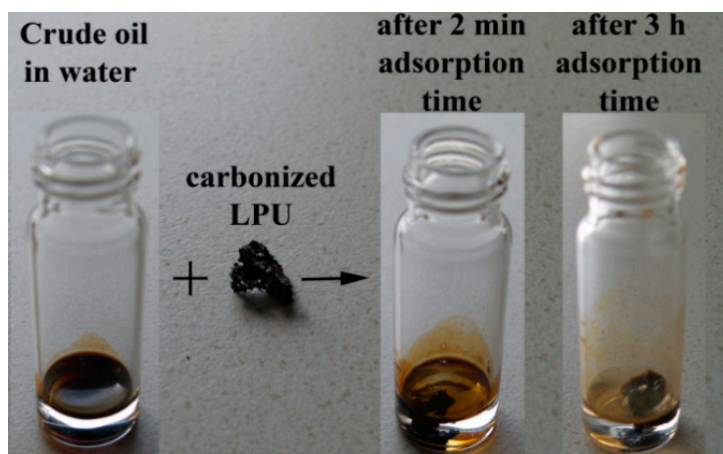


**Figure 6.** Crude oil adsorption ability of carbonized LPU 2.

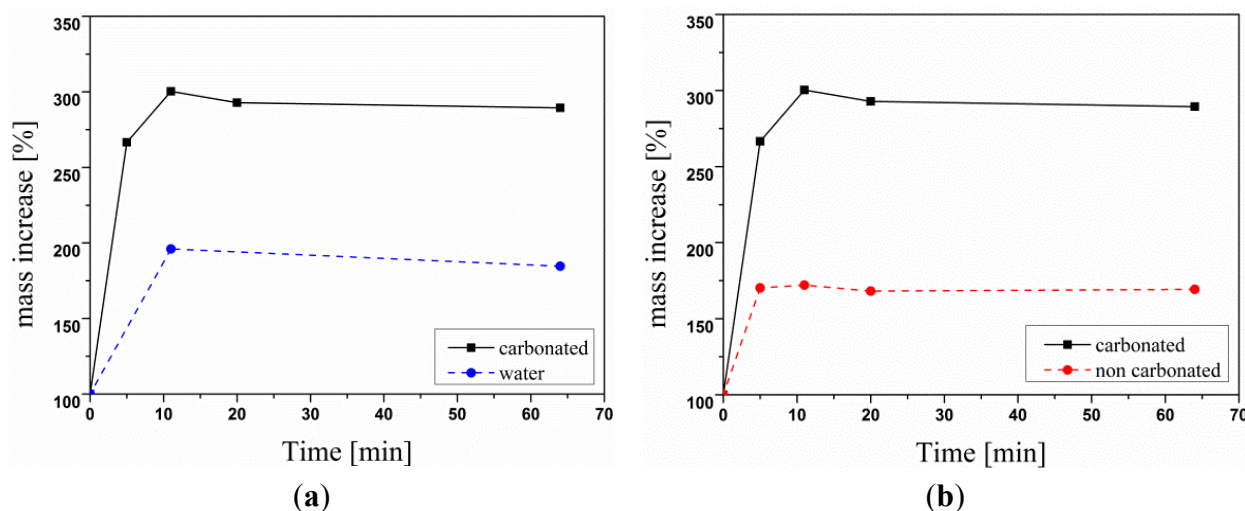


**Figure 7.** Oil uptake of carbonated LPU compared to the uptake of water (a) and the uptake of crude oil from the carbonated LPU compared to the non-carbonated species (b).

### 3. Experimental Section

#### 3.1. Material

Lignin (Indulin AT, Sigma Aldrich, Steinheim, Germany) and sodium lignosulfonate (Sigma Aldrich, Steinheim, Germany), as well as the cross-linker toluene 2,4-diisocyanate (TDI, 96%, Sigma Aldrich, Steinheim, Germany) were used without further purification. In this study, lignin cross-linked with TDI is called lignin-polyurethane (LPU), while sodium lignosulfonate cross-linked with TDI is called lignosulfonate-polyurethane (LSPU). The Kraft lignin Indulin AT and a sodium lignosulfonate were

used to produce carbon materials. All raw materials were characterized by elemental analysis. The sulfur content in the lignosulfonate determined by elemental analysis constitutes the sulfonate content in the raw material. Unlike for lignin, the lignosulfonates investigated contain sodium, which cannot be detected with the elemental analysis method and which is thus unaccounted for in the elemental analysis results. Consequentially, absolute results from elemental analysis have a deviation, while relations between the individual elements can correctly be made and constitute a relative composition.

In order to receive definable structures from the reaction of lignin and lignosulfonates with diisocyanates, no additional catalyst was used for the cross-linking reaction. The reactivity of the functional groups of the reactants was studied with model substances as discussed in the next section. The cross-linker toluene-2,4-diisocyanate (TDI) was chosen since its aromatic structure fits into the lignin base structure.

### 3.1.1. Cross-Linking Reaction Study

The cross-linking reaction was studied with the model substances phenol (>99%, for synthesis, Merck, Darmstadt, Germany), anisole (99%, Merck), benzylalcohol (for analysis, Merck), 4-hydroxybenzyl alcohol (HBA, >98%, Sigma-Aldrich), 4-hydroxy-3-methoxybenzyl alcohol (VA, vanillyl alcohol, 98%, Alfa Aesar, Karlsruhe, Germany), 4-hydroxy-3,5-dimethoxybenzyl alcohol (SA, syringyl alcohol, 97%, Alfa Aesar, Karlsruhe, Germany), methanesulfonic acid (purum, >98%, Fluka, Steinheim, Germany) and sodium methanesulfonate (produces by neutralizing methanesulfonic acid with sodium hydroxide and drying). Therefore, a certain amount of the model substance was first dissolved in a deuterated solvent (non-sulfonated in  $\text{CDCl}_3$  ( $\geq 99.8\%$ , for NMR spectroscopy, Merck, Darmstadt, Germany), sulfonated in dimethyl sulfoxide (DMSO,  $\geq 99.8\%$ , for NMR-spectroscopy, Merck, Darmstadt, Germany) and then TDI was added in a specific molar ratio. The solution was kept at 60 °C for 10 min, measured by NMR spectroscopy (see below) and kept at 60 °C for another 24 h. After a second NMR measurement, the catalyst N,N,N',N'-tetramethylethylenediamine (TEMED, p.a., Merck, Darmstadt, Germany) was added and after 10 min at 60 °C, the sample was measured by NMR spectroscopy again.

### 3.1.2. Production of LPU and LSPU

For the synthesis of LPU and LSPU, no solvent was used, only the lignin source and TDI. The base materials were thoroughly mixed in a sealable glass vessel and subsequently put inside an oven at 60 °C. After 24 h reaction time, the material was taken out and put into ceramic containers for further pyrolysis.

The resulting polyurethanes were measured by FT-IR spectroscopy. Figure 8 shows the spectra of the lignin starting material and one resulting lignin polyurethane. The product shows new absorption bands at  $3304.82\text{ cm}^{-1}$  which can be attributed to the N-H stretching, and also at  $1712.61\text{ cm}^{-1}$ , which can be attributed to the carbonyl group. The absorption band at  $2260.17\text{ cm}^{-1}$  is formed by the unreacted isocyanate group [37].

### 3.1.3. Carbonization Reaction

The carbonization of the materials was performed in a "GERO HTK8" high-temperature oven. The following temperature program was used: from room temperature to 500 °C with a heating rate of

$1\text{ }^{\circ}\text{C}\cdot\text{min}^{-1}$ . This temperature was held for 1 h and was then increased to  $900\text{ }^{\circ}\text{C}$  with a rate of  $5\text{ }^{\circ}\text{C}\cdot\text{min}^{-1}$ . The carbonization temperature was held for 2 h. The whole procedure was performed under a nitrogen flow of  $150\text{ L}\cdot\text{h}^{-1}$ .

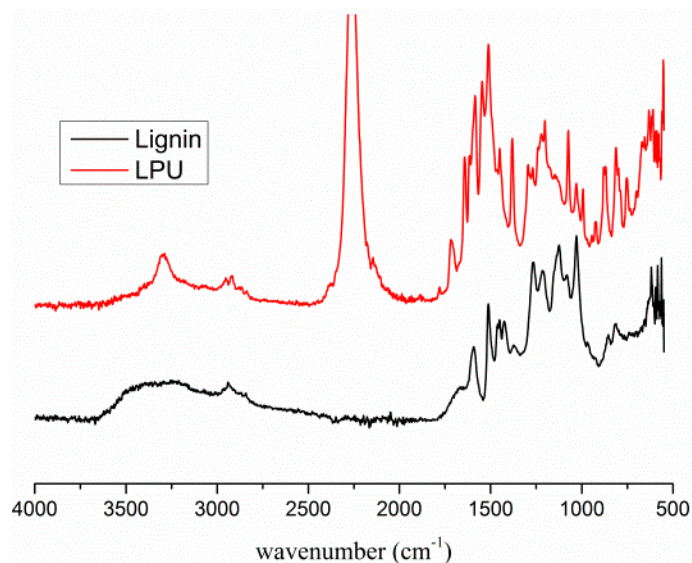


**Figure 8.** Comparison of FT-IR spectra of starting material (lower spectra) and resulting lignin polyurethane (upper spectra).

### 3.2. General Measurements

#### 3.2.1. NMR Spectroscopy

A Bruker digital Avance III 300 MHz NMR-spectrometer was used.  $^1\text{H}$  NMR measurements were performed for reactions of the model substances, which were dissolved in  $\text{CDCl}_3$  and in DMSO, respectively.

#### 3.2.2. Elemental Analysis

For elemental analysis, a Thermo FlashEA 1112 CHNS-O analyzer with sulfanilamide as a standard substance was used. Samples were weighed on a Mettler UMT2 balance.

#### 3.2.3. Scanning Electron Microscopy

Scanning electron microscopy (SEM) analysis was performed on a Zeiss 1540XB CrossBeam equipped with an Oxford Instruments EDX system. The electrical high tension (EHT) was set to 5 kV and different magnifications were used for measurements.

#### 3.2.4. BET Surface Area Determination

BET surface was determined using a Quantachrome Nova 3000e analyzer. Only multi-point BET analysis necessary adsorption points were determined. Prior to the analysis, the sample materials were degassed under high vacuum for 1 h at  $200\text{ }^{\circ}\text{C}$ .

### 3.2.5. FT-IR-Spectroscopy

The IR absorption was measured on a Thermo-Scientific Nicolet 5700 FT-IR spectrometer mounted with a Thermo Foundation ATR.

### 3.2.6. Crude Oil Adsorption Test

50 mg of crude oil for the crude oil adsorption test were added to 450 mg of water. Subsequently, pieces of about 100 mg of the carbonized material were cut and weighed exactly. Each of these was added to one of the oil-water mixtures. These were shaken for 2 min and further to 3 h before photographic documentation. The uptake of oil was registered by a balance after 5, 10, 20 and 65 min. A blind control was performed with a non-carbonized material.

## 4. Conclusions

Carbon materials were produced via isocyanate cross-linking of lignin and lignosulfonate and a subsequent carbonization reaction. For the cross-linking reaction, it was shown with model substances that without a catalyst, lignin predominately cross-links via its aliphatic OH groups, while sulfonate groups of lignosulfonates act as a catalyst. The model reaction studies could confirm former studies on the reactivity of OH groups and different isocyanates [27]. It could also be shown that the H-lignin model would be more reactive than the G- and S-lignin models.

The cross-linking degree constitutes the final surface area and structure, while intermediate cross-linking results in the highest surface areas and roughest structures. Lignosulfonates form nano-sized salt crystals on its surface after carbonization, which absorb water and causes sinking. In contrast, Kraft lignin polyurethanes float in water and have a good ability to adsorb crude oil.

## Supplementary Materials

Supplementary materials can be found at <http://www.mdpi.com/2311-5629/1/01/43/s1>.

## Acknowledgments

The work was performed under the BioPol project, which is funded by the European Regional Development Fund (EFRE) and the province of Upper Austria. The NMR experiments were performed at the Upper Austrian–South Bohemian Research Infrastructure Center in Linz, co-financed by the European Union in the context of the project “RERI-uasb”, EFRE RU2-EU-124/100-2010 (ETC Austria-Czech Republic 2007–2013, project M00146). Special thanks go to DI(FH) Günter Hesser (CSNA Center for Surface- and Nanoanalytics, Johannes Kepler University Linz) for performing SEM measurements.

## Author Contributions

Sebastian Leitner and Günther Gratzl performed the experiments, analyzed the data, created the Figures, and wrote the manuscript. Hedda Weber and Christina Paulik supervised the project and helped with interpreting the data.

## Conflicts of Interest

The authors declare no conflict of interest.

## References

1. Laurichesse, S.; Avérous, L. Chemical modification of lignins: Towards biobased polymers. *Prog. Polym. Sci.* **2014**, *39*, 1266–1290.
2. Ragauskas, A.J.; Beckham, G.T.; Bidy, M.J.; Chandra, R.; Chen, F.; Davis, M.F.; Davison, B.H.; Dixon, R.A.; Gilna, P.; Keller, M.; *et al.* Lignin Valorization: Improving Lignin Processing in the Biorefinery. *Science* **2014**, *344*, doi:10.1126/science.1246843.
3. Baker, D.A.; Rials, T.G. Recent advances in low-cost carbon fiber manufacture from lignin. *J. Appl. Polym. Sci.* **2013**, *130*, 713–728.
4. Maradur, S.P.; Kim, C.H.; Kim, S.Y.; Kim, B.-H.; Kim, W.C.; Yang, K.S. Preparation of carbon fibers from a lignin copolymer with polyacrylonitrile. *Synth. Met.* **2012**, *162*, 453–459.
5. Hu, K.; Kulkarni, D.D.; Choi, I.; Tsukruk, V.V. Graphene-polymer nanocomposites for structural and functional applications. *Prog. Polym. Sci.* **2014**, *39*, 1934–1972.
6. Trigueiro, J.P.; Lavall, R.L.; Silva, G.G. Supercapacitors based on modified graphene electrodes with poly(ionic liquid). *J. Power Sources* **2014**, *256*, 264–273.
7. German, R.; Venet, P.; Sari, A.; Briat, O.; Vinassa, J.-M. Improved Supercapacitor Floating Ageing Interpretation Through Multipore Impedance Model Parameters Evolution. *IEEE Trans. Power Electron.* **2014**, *29*, 3669–3678.
8. Worsley, M.A.; Pauzauskie, P.J.; Olson, T.; Biener, J.; Satcher, J.H., Jr.; Baumann, T.F. Synthesis of Graphene Aerogel with High Electrical Conductivity. *J. Am. Chem. Soc.* **2010**, *132*, 14067–14069.
9. Ou, Y.-J.; Peng, C.; Lang, J.-W.; Zhu, D.-D.; Yan, X.-B. Hierarchical porous activated carbon produced from spinach leaves as an electrode material for an electric double layer capacitor. *New Carbon Mater.* **2014**, *29*, 209–215.
10. Torres, J.A.; Kaner, R.B. Graphene synthesis: Graphene closer to fruition. *Nat. Mater.* **2014**, *13*, 328–329.
11. Reddy, K.S.; Shoaibi, A.A.; Srinivasakannan, C. A comparison of microstructure and adsorption characteristics of activated carbons by CO<sub>2</sub> and H<sub>3</sub>PO<sub>4</sub> activation from date palm pits. *New Carbon Mater.* **2012**, *27*, 344–351.
12. Fraccarollo, A.; Canti, L.; Marchese, L.; Cossi, M. Monte Carlo Modeling of Carbon Dioxide Adsorption in Porous Aromatic Frameworks. *Langmuir* **2014**, *30*, 4147–4156.
13. Wu, S.; Liu, Y.; Yu, G.; Guan, J.; Pan, C.; Du, Y.; Xiong, X.; Wang, Z. Facile Preparation of Dibenzoheterocycle-Functional Nanoporous Polymeric Networks with High Gas Uptake Capacities. *Macromolecules* **2014**, *47*, 2875–2882.
14. Kuzmich, D.; Coupillaud, P.; Men, Y.; Vignolle, J.; Vendramineto, G.; Ambrogi, M.; Taton, D.; Yuan, J. Functional mesoporous poly(ionic liquid)-based copolymer monoliths: From synthesis to catalysis and microporous carbon production. *Polymer* **2014**, *55*, 3423–3430.
15. Duan, L.-Q.; Ma, Q.-S.; Chen, Z.-H. The production of high surface area porous carbonaceous materials from polysiloxane. *New Carbon Mater.* **2013**, *28*, 235–240.

16. Mansouri, N.-E.E.; Yuan, Q.; Huang, F. Characterization of alkaline lignins for use in phenol-formaldehyde and epoxy resins. *Bioresources* **2011**, *6*, 2647–2662.
17. Shen, Q.; Zhang, T.; Zhang, W.-X.; Chen, S.; Mezgebe, M. Lignin-based activated carbon fibers and controllable pore size and properties. *J. Appl. Polym. Sci.* **2011**, *121*, 989–994.
18. Mansouri, N.-E.E.; Pizzi, A.; Salvado, J. Lignin-based polycondensation resins for wood adhesives. *J. Appl. Polym. Sci.* **2007**, *103*, 1690–1699.
19. Muller, P.C.; Kelley, S.S.; Glasser, W.G. Engineering Plastics from Lignin. IX. Phenolic Resin Synthesis and Characterization. *J. Adhes.* **1984**, *17*, 185–206.
20. Hatakeyama, H.; Nakayachi, A.; Hatakeyama, T. Thermal and mechanical properties of polyurethane-based geocomposites derived from lignin and molasses. *Compos. Part A—Appl. Sci.* **2005**, *36*, 698–704.
21. Hatakeyama, T.; Matsumoto, Y.; Asano, Y.; Hatakeyama, H. Glass transition of rigid polyurethane foams derived from sodium lignosulfonate mixed with diethylene, triethylene and polyethylene glycols. *Thermochim. Acta* **2004**, *416*, 29–33.
22. Hatakeyama, T.; Asano, Y.; Hatakeyama, H. Mechanical and thermal properties of rigid polyurethane foams derived from sodium lignosulfonate mixed with diethylene-, triethylene- and polyethylene glycols. *Macromol. Symp.* **2003**, *197*, 171–180.
23. Chung, H.; Washburn, N.R. Improved Lignin Polyurethane Properties with Lewis Acid Treatment. *ACS Appl. Mater. Interfaces* **2012**, *4*, 2840–2846.
24. Ismail, T.N.; Hassan, H.A.; Hirose, S.; Taguchi, Y.; Hatakeyama, T.; Hatakeyama, H. Synthesis and thermal properties of ester-type crosslinked epoxy resins derived from lignosulfonate and glycerol. *Polym. Int.* **2009**, *59*, 181–186.
25. Wohlmann, B.; Woelki, M.; Ebert, A.; Engelmann, G.; Fink, H.P. Lignin Derivative, Shaped Body Comprising the Derivative, and Carbon Fibers Produced from the Shaped Body. WO 2010081775 A1, 22 July 2010.
26. Yamaji, T.; Saito, T.; Hayamizu, K.; Yanagisawa, M.; Yamamoto, O. Spectral Database for Organic Compounds, SDBS. Available online: <http://sdb.sdb.aist.go.jp> (accessed on 25 September 2014).
27. Zhuang, J.M.; Steiner, P.R. Thermal reactions of diisocyanate (MDI) with phenols and benzylalcohols: DSC study and synthesis of MDI adducts. *Holzforsch.—Int. J. Biol. Chem. Phys. Technol. Wood* **1993**, *47*, 425–434.
28. Brudin, S.; Schoenmakers, P. Analytical methodology for sulfonated lignins. *J. Sep. Sci.* **2010**, *33*, 439–452.
29. Chen, X.Y.; Zhou, Q.Q. The production of porous carbon from calcium lignosulfonate without activation process and the capacitive performance. *Electrochim. Acta* **2012**, *71*, 92–99.
30. Zhang, W.-J.; Li, T.-H.; Lu, M.; Hou, C.-L. A comparative study of the characteristics and carbonization behaviors of three modified coal tar pitches. *New Carbon Mater.* **2013**, *28*, 140–144.
31. Liu, Q.; Wang, S.; Zheng, Y.; Luo, Z.; Cen, K. Mechanism study of wood lignin pyrolysis by using TG-FTIR analysis. *J. Anal. Appl. Pyrolysis* **2008**, *82*, 170–177.
32. Grønli, M.G.; Várhegyi, G.; di Blasi, C. Thermogravimetric Analysis and Devolatilization Kinetics of Wood. *Ind. Eng. Chem. Res.* **2002**, *41*, 4201–4208.
33. Brebu, M.; Tamminen, T.; Spiridon, I. Thermal degradation of various lignins by TG-MS/FTIR and Py-GC-MS. *J. Anal. Appl. Pyrolysis* **2013**, *104*, 531–539.

34. Li, B.; Lv, W.; Zhang, Q.; Wang, T.; Ma, L. Pyrolysis and catalytic pyrolysis of industrial lignins by TG-FTIR: Kinetics and products. *J. Anal. Appl. Pyrolysis* **2014**, *108*, 295–300.
35. Wu, H.; Fan, S.-W.; Yuan, X.-W.; Chen, L.-F.; Deng, J.-L. Fabrication of carbon fibers from jute fibers by pre-oxidation and carbonization. *New Carbon Mater.* **2013**, *28*, 448–453.
36. Okiel, K.; El-Sayed, M.; El-Kady, M.Y. Treatment of oil-water emulsions by adsorption onto activated carbon, bentonite and deposited carbon. *Egypt. J. Pet.* **2011**, *20*, 9–15.
37. Zhang, H.; Chen, Y.; Zhang, Y.; Sun, X.; Ye, H.; Li, W. Synthesis and characterization of polyurethane elastomers. *J. Elastom. Plast.* **2008**, *40*, 161–177.

© 2015 by the authors; licensee MDPI, Basel, Switzerland. This article is an open access article distributed under the terms and conditions of the Creative Commons Attribution license (<http://creativecommons.org/licenses/by/4.0/>).